

# THE STIFFNESS OF UNSATURATED RAILWAY FORMATION

L. Otter <sup>1</sup>

C.R.I. Clayton <sup>2</sup>

J.A. Priest <sup>3</sup>

P.J. Gräbe <sup>4</sup>

<sup>1</sup> Formerly University of Southampton, UK

<sup>2</sup> University of Southampton, UK

<sup>3</sup> University of Calgary, Canada, formerly University of Southampton, UK

<sup>4</sup> University of Pretoria, South Africa, [Hannes.grabe@up.ac.za](mailto:Hannes.grabe@up.ac.za)

## ABSTRACT

The rational design of rail substructure requires estimates of the stiffnesses of the formation on which it is to be built. Stiffnesses derived from back-analyses of deformations of the ground beneath rail track have been found by the authors to be much higher than those predicted from laboratory element testing on saturated specimens. This may be because of differences in compaction between field and laboratory, or because suctions created by lack of saturation play a key role in controlling stiffness, and therefore the performance of the track when in use.

To test the latter hypothesis a laboratory study has been carried out on material representative of that found in South African railway formations. This was tested at constant dry density and various water contents, with matric suctions determined using different established techniques, and very small strain stiffness obtained from resonant column testing. A suction stress characteristic curve (SSCC) was developed to identify the contribution of suction to the overall effective stress for this material.

The results show that suction can indeed be an important contributing factor for stiffness. For material tested at constant dry density, stiffness initially increases with reducing compaction water content, and therefore with increasing suction. It subsequently reduces back towards the saturated value as the compaction water

content approaches zero, even though the matric suction continues to increase. The relative increase in very small strain stiffness due to suction depends to a large extent on the net normal stress during stiffness measurement. The effect of matric suction is proportionately greatest at the low net normal stress levels that apply for shallow infrastructure such as rail formations. And the operational stiffness depends not only on the current water content (and therefore suction), but also on the water content at which the material has been compacted.

**Keywords:** railway track, formation stiffness, suction, unsaturated soils, railway track design,

## INTRODUCTION

Modern “structural” rail track design uses theory-based methods to calculate stresses and strains at key points in the pavement structure. These are then used to determine the necessary thickness of the individual road or rail substructure layers, and to predict the permanent deflections under traffic loading. “Mechanistic-empirical” methods of design, as these are termed, therefore require estimates of the resilient moduli and permanent strains that will occur in the various materials, including the formation and the underlying common fill or natural ground [1].

In the absence of laboratory measurements of stiffness for a given project, resilient modulus can be estimated on the basis of empirical relationships [2]. The success of such correlations relies on the selection of the dominant factors controlling stiffness, for example density and water content. This paper aims to improve future mechanistic-empirical design by exploring the effect of suction on resilient modulus.

The determination of the stiffness of formation materials is a challenge. Such materials are typically relatively coarse compared with the underlying soils, have been heavily compacted, are unsaturated, operate under low ambient effective stress levels, and are subject to complex dynamic and cyclic loading involving principal stress rotation (PSR) [3]. In previous studies the authors have assessed the effects of initial stress, over-consolidation and PSR on the permanent strains and

resilient moduli of a range of saturated materials tested in the laboratory cyclic hollow cylinder apparatus [3][4]. In comparison with stiffnesses used for South African heavy-haul track design [5], and stiffnesses determined from back-analysis of track monitoring [6], the stiffnesses determined in our laboratory cyclic hollow cylinder testing were found to be relatively low. This may be for a number of reasons:

- The laboratory tests were carried out under saturated, constant volume conditions while in the field the materials were under unsaturated conditions. An unsaturated state will permit volume change during train loading. In addition, matric suctions (which are not present in a saturated material) could potentially increase stiffness.
- The materials at the field test section were subjected to high levels of vibratory compaction, to ensure that the target dry densities (90% to 98% of Modified AASHTO maximum, depending on the layer) were met. This method of compaction could result in relatively high stiffnesses compared to those produced by laboratory consolidation in the hollow cylinder apparatus.

In previous research [2], a model was developed based on the assumption that the resilient modulus of fine-grained subgrade is related to the difference between the optimum moisture content and the field moisture content of the material. Empirical equations were developed to quantify these relationships for constant dry density and constant compactive effort. For both cases it was concluded that drier than optimum moisture conditions would result in higher resilient modulus and lower resilient modulus for wetter than optimum moisture conditions.

This paper explores the effect of lack of saturation on the very small strain stiffness,  $G_0$ , of a formation material, using the resonant column apparatus.

## **METHODOLOGY**

This section describes the material used in our tests, the methods of preparation of specimens, and the determination of stiffness and matric suction for these materials.

### ***Selection of representative material***

The range of materials used for various layers in rail track bed, based on a survey carried out over the 650 km heavy haul South African Coal Line has previously been reported [4]. Track construction in South Africa (Figure 1) uses four 200-mm thick layers below the ballast: Special Subballast, Subballast, Class A subgrade, and Class B subgrade. Below this lies either natural ground or bulk earthworks. Four materials (termed Materials A, B, C and D) were previously selected [4] to represent these layers during hollow cylinder testing.

The testing described in this paper was carried out on Material B, a clayey sand containing 11% clay, that represents the Class A Subgrade material between 400 mm and 600 mm below the Subballast. During design, the target resilient Young's modulus for this layer was 100 MPa. In a monitored full-scale field trial [6] the average back-figured resilient Young's modulus of this layer was reported to be 182 MPa.

### ***Choice of dry density and water contents***

On the basis of previous research [7][8] it was expected that important contributors to the stiffness of rail formation materials would be:

- Net normal stress, resulting from stresses imposed by sleepers, ballast and upper formation levels.
- Matric suction caused by lack of saturation in rail formation itself.
- The dry density achieved by compaction.

Experimental determinations of the matric suctions in clayey sands [9] suggest that contours of matric suction, when plotted on axes of dry density v. water content, lie approximately parallel to the dry density axis. Dry density can be expected to have relatively little effect on suction, except near the saturation (zero air voids) line. In order to explore the effect of lack of saturation while minimising the effect of dry density on measured stiffness, the decision was made to test the material compacted to a single target dry density at a range of water contents.

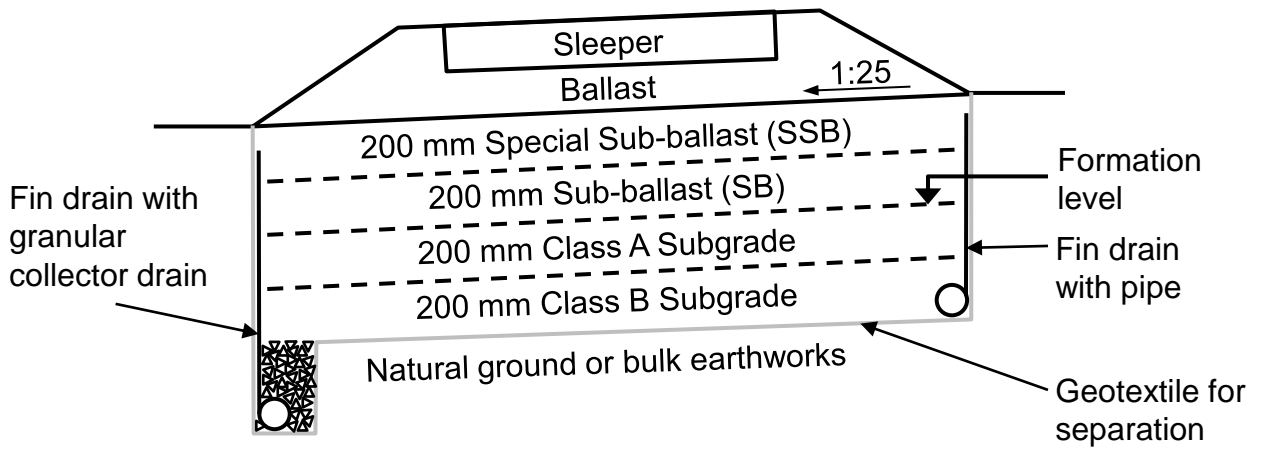


Figure 1. Cross section through upgraded South African heavy haul rail track

Laboratory compaction tests were carried out on Material B. The maximum dry densities and associated optimum water contents are shown in Table 1. The effect of differences in compactive effort can be assessed from the results of 2.5 kg and 4.5 kg rammer tests on Material B. It can be seen that, as expected, a significant increase in maximum dry density and decrease of optimum water content occurs when compactive effort is increased. The effect of specimen geometry was assessed by preparing the 70 mm diameter by 140 mm high specimens required for subsequent stiffness testing using the same energy input per unit volume as in the 2.5 kg rammer test .

**Table 1. Laboratory compaction test results for Materials B (Tests to BS 1377 part 4 (1990)), equivalent to AASHTO T99 (5.5lb rammer) and T180 (10lb rammer).**

Max. dry density (Mg/m <sup>3</sup> ) / Optimum water content (%)		
2.5 kg rammer	Modified 2.5 kg [1] rammer	4.5 kg rammer
2.17 / 6.8	2.10 / 8.0	2.26 / 4.6

Note 1. 70 mm dia. x 140 mm high specimens compacted with 15 blows / layer, in three layers.

On the basis of the laboratory compaction test data discussed above, and on the results of laboratory compaction tests and field density tests carried out on a 34 km section of railway track on the South Africa Coal Line that had been reconstructed in 2002, a target dry density of 2.10 Mg/m<sup>3</sup> was adopted for stiffness measurements on Material B. For the material tested in the laboratory (specific gravity = 2.62 to 2.64) the limiting (saturated) water content is approximately 10% at a dry density of 2.10 Mg/m<sup>3</sup>.

### ***Preparation of specimens for stiffness measurement***

70 mm diameter x 140 mm high specimens were prepared using Proctor compaction, i.e. using a 2.5 kg rammer falling through 300mm. During initial testing the number of layers per specimen was varied, in order to examine specimen uniformity, and the number of blows was modified accordingly, to maintain the energy / unit volume at the standard value (approximately 600 kJ/m<sup>3</sup>). Comparison of two specimens prepared at 8% water content to a dry density of 2.10 Mg/m<sup>3</sup>, with one built of three layers and the other of ten, showed that at any net normal stress the difference in shear modulus was no greater than 7%, so within the repeatability of stiffness measurements. However, in order to reduce density variations due to layering within the specimens, it was decided to compact the specimens in ten layers.

The results of compaction on Material B were explored using an X-TEK / Nikon Metrology HMX ST computed tomography scanner at the University of Southampton. With the specimen scanned in two (upper and lower) sections, the voxel resolution was 44.6 µm. The output from the CT scanner was calibrated by assuming a straight line relationship between digital number and the densities of quartz, clay, plastic billets, and air, scanned alongside the compacted specimen. The data provided an estimate of the bulk density of the compacted material.

A simple radiograph (Figure 2) showed some evidence of layering, even when 10 layers were used for each specimen. Also, not unexpectedly [10], a significantly higher average bulk density (of the order of 0.3 Mg/m<sup>3</sup>) was measured at the base of the specimen than at the top. This gives rise to the apparent upward reduction of the specimen cross section shown in Figure 2.

Also of note was the fact that despite best efforts to evenly distribute the various grain sizes (and particularly the clay) throughout the specimen, CT sections showed clear evidence of zones that were clay rich, and those that appeared essentially coarse and granular (Figure 3).

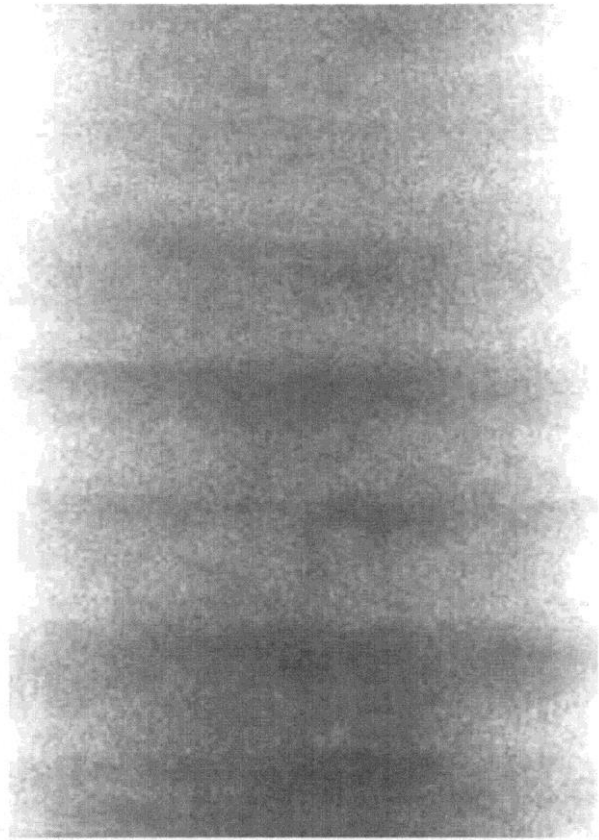


Figure 2. Radiograph of bottom two-thirds of a compacted specimen of Material B, bulk density =  $2.18 \text{ Mg/m}^3$ , dry density =  $2.10 \text{ Mg/m}^3$ , water content = 4.2%



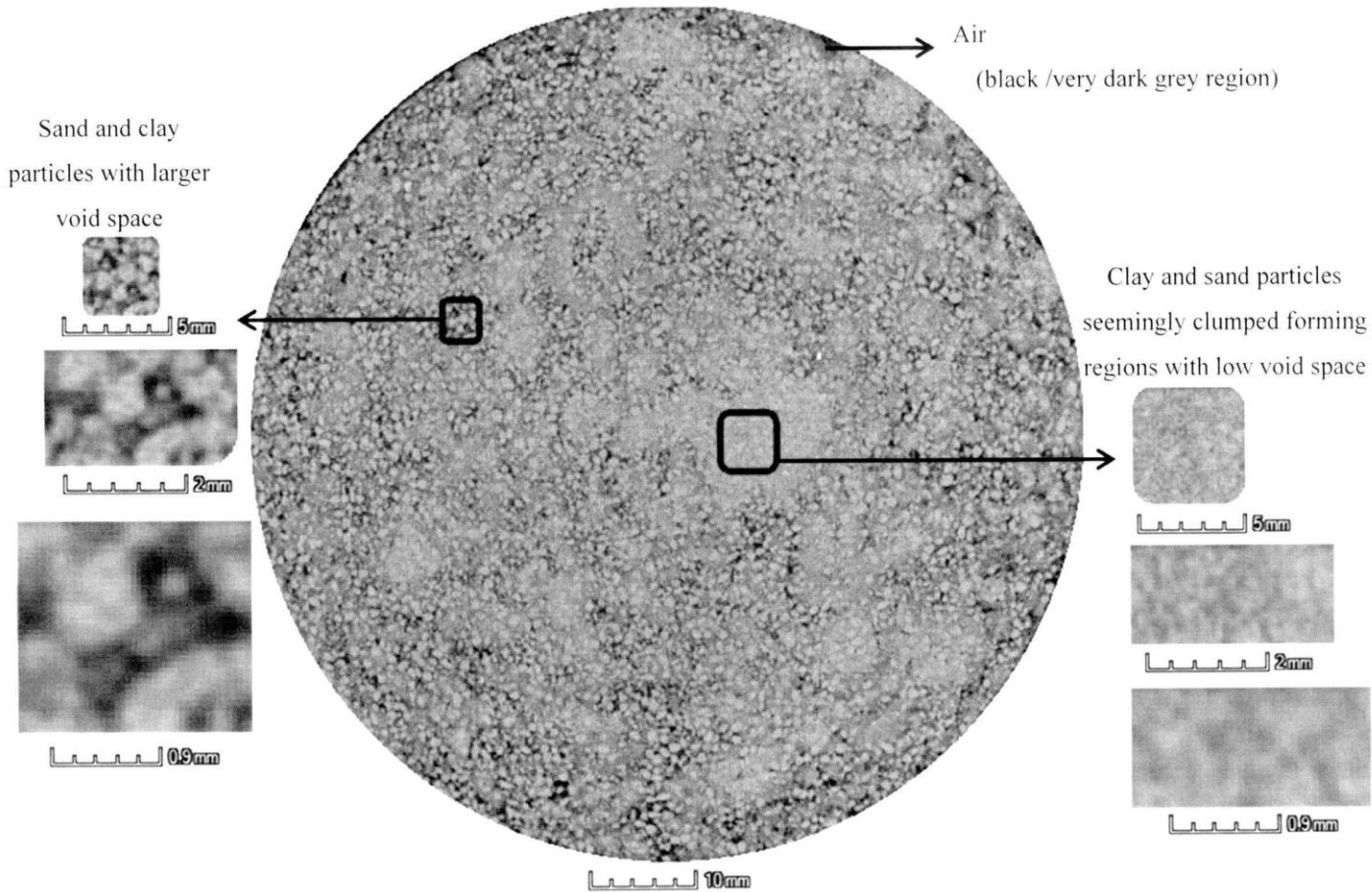


Figure 3. CT reconstruction of a horizontal section through a compacted specimen of material B, showing areas with coarse and fine textures.

### ***Determination of very small strain stiffness***

In this study very small strain stiffness,  $G_0$ , was used as a proxy for operational stiffness which, because of higher strain levels, can be expected to be lower than  $G_0$ . A fixed-free Stokoe resonant column apparatus [11] was used to determine  $G_0$  of the compacted material. Calibration and determination of apparatus constants was carried out using a set of four solid aluminium calibration bars [12]. 70 mm diameter x 140 mm specimens were tested with the back pressure line open to atmosphere, and with an air cell pressure that was varied in order to measure stiffness under a range of net normal stress. After the application of each net normal stress the resonant frequency of the specimen was measured at two-hourly intervals, at very small strain, in order to monitor the effects of creep on stiffness, and to ensure that equalisation had occurred under the applied pressures. After twenty four hours the very small strain shear modulus was measured. The net normal stress was then increased, and the process repeated. The results reported in this paper are for specimens tested under net normal stresses that varied between 10 kPa and 150 kPa.

A total of 21 specimens of Material B were prepared to a target dry density of  $2.10 \text{ Mg/m}^3$ , with water contents between 2% and 10%, and were then tested for stiffness at their as-prepared water contents. Five further specimens of Material B were prepared at water contents between 6% and 10%, and were then air dried, before being tested for stiffness at a range of net normal stress.

### ***Determination of matric suction and soil-water characteristic curves***

Because of the potential difficulties in measuring pore air and pore water pressures in the resonant column apparatus, matric suction was determined separately, on duplicates of the specimens used in stiffness measurement. Three methods of matric suction measurement were used:

- The filter paper technique [13][14]
- The pressure-plate apparatus [15]
- A suction probe [16]

For the filter paper technique, Whatman No. 42 filter paper [17] was used in contact with the soil. The results were interpreted using Chandler et al.'s wetting calibration curve [18]. For each filter paper test, two 20 mm high full diameter specimens were cut from a sacrificial 70 mm diameter resonant column specimen (see above), and the cut surfaces were smoothed to ensure good contact with the filter paper that would later be placed on them. The two sections were then combined and weighed.

The filter papers were wetted in a purpose-built tank containing a pond fogger, over a period of between eight and sixteen hours. The two halves of the specimen were then split, and three wetted filter papers were placed centrally on one half, using tweezers. The other half of the specimen was then placed on top, and the combined specimen was sealed using insulating tape to prevent water loss. The specimen was then placed in a sealed close-fitting glass container, in an insulated polystyrene box. This was stored at 20 °C for seven days, to allow water equalisation between the specimen and the filter paper. After seven days the specimen was removed from the box, and the water content of the central filter paper was determined [14][15].

The soil water characteristic curve of the material was also determined using the pressure plate apparatus. Two apparatus were used, one with a 500 kPa high-air-entry disc, and the other housing a 1500 kPa high-air-entry disc. After some experimentation, pressure loading stages from 10 – 500 kPa, each of 1 day duration, were used for the 500 kPa apparatus, whilst loading stages of 80 – 1500 kPa with periods of four days were used for the 1500 kPa apparatus, to ensure that equilibrium was reached. Tests were conducted on 65 mm diameter, 20 mm high sub-sections of unsaturated materials, made using the technique adopted for the 70 mm x 140 mm resonant column apparatus specimens. The pressure plate specimens were sampled by pushing cutter rings into the larger specimens, and carefully trimming their ends. This technique, and the use of small weights (130 g) placed centrally on the top of the specimens, ensured good contact between the soil and the high entry discs. After each time period, air pressure was reduced, and a specimen was removed and weighed before drying to determine its water content. The apparatus was immediately re-sealed and the next pressure stage applied.

For the purpose of comparison, measurements were also made on a number of specimens using a suction probe [19]. These were prepared to the same dry density

and water content as those tested in the resonant column apparatus, using the same Proctor compaction rammer, but were compacted into plastic tube moulds to produce specimens 77 mm diameter and 120 mm high. The suction probe was lightly spring mounted in a base platen. The top sealing of the plastic mould was removed and the exposed specimen surface was then placed directly on the base platen and probe. A soft kaolin paste was used to ensure good contact. The material was then re-sealed and the response of the instrument was measured for 24 hours, the maximum recorded value being taken as the suction.

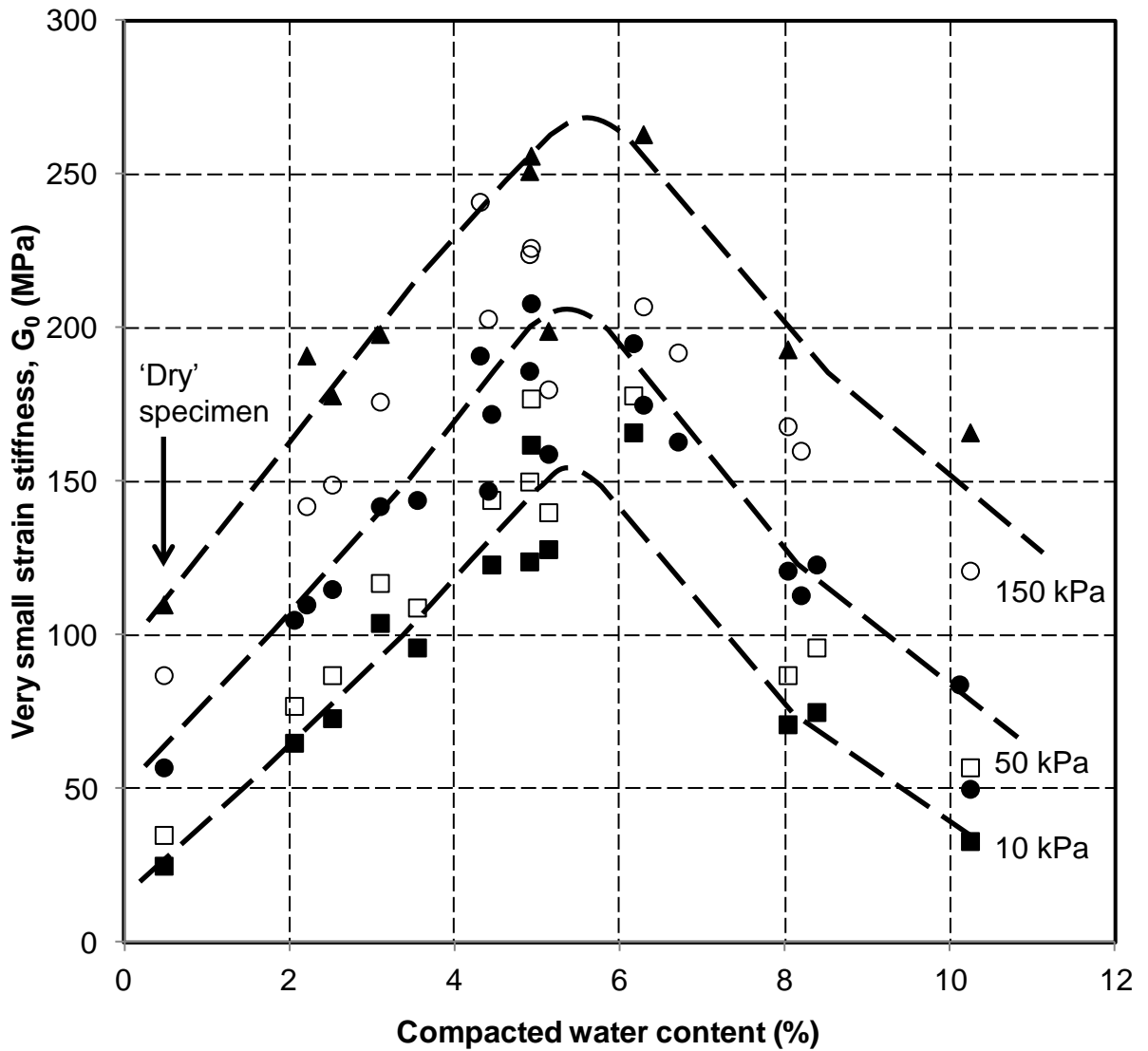
## **DISCUSSION**

This section brings together the results of our stiffness testing, and where appropriate compares them with previous estimates of the stiffness of saturated rail formation materials, made for example using the cyclic hollow cylinder apparatus, and derived from back-analysis of field measurements. It then estimates the magnitude of matric suctions in the tests, and explores the impact of these on observed stiffness behaviour using the suction stress approach [20]. Finally, implications for practice are discussed.

### ***The effects of saturation on stiffness***

Figure 4 shows very small strain shear modulus ( $G_0$ ) data for specimens of Material B tested with a specimen target dry density of  $2.10 \text{ Mg/m}^3$  at a range of compaction water contents. It will be recalled that a specimen with a water content of 10% and a dry density of  $2.10 \text{ Mg/m}^3$  will be 100% saturated; one with zero water content will be 0% saturated.

The results shown in Figure 4 are for specimens tested at the same water contents at which they had been compacted. Each specimen was tested under a range of net normal stresses, created by applying a cell pressure with the apparatus back pressure line vented to atmosphere. In order to ensure that the specimen pore air pressure equilibrated with the (atmospheric) back pressure, each cell pressure was held until regular resonant column tests showed that stiffness change had ceased.



- Net normal stress = 10kPa
- Net normal stress = 20kPa
- Net normal stress = 50kPa
- Net normal stress = 100 kPa
- ▲ Net normal stress = 150kPa

Figure 4. Very small strain shear modulus of Material B, compacted and tested at a range of water contents.

It can be seen that the measured very small strain stiffness,  $G_0$ , of Material B varies between approximately 25 MPa and 260 MPa. Assuming isotropy and a Poisson's ratio of 0.25, this is equivalent to a Young's modulus variation from 60 MPa to 650 MPa. These results seem reasonable when compared with

- Resilient modulus values between 200 MPa and 1000 MPa obtained from cyclic triaxial testing [21] for an unsaturated granular highway pavement material tested at two target water contents.
- Resilient modulus values of 60 - 70 MPa measured on saturated cyclic hollow cylinder specimens of rail formation material [4].
- A track design target value of resilient Young's modulus of 100 MPa [5], and
- A resilient Young's modulus back-figured from field monitoring of rail track in South Africa of 182 MPa [6].

Because the resonant column apparatus measures stiffness at very small strains, the values obtained from it might be expected to be higher than the stiffnesses measured, for example, at higher strain levels in the cyclic triaxial or cyclic hollow cylinder apparatus.

Trend lines superimposed on the data in Figure 4 show, despite the scatter of data, that water content (and therefore degree of saturation) has a large impact on small strain stiffness. It can be estimated, for example, that at zero net normal stress a specimen would have virtually no stiffness when dry (0% water content) and when saturated (10% water content), but would have a considerable stiffness ( $G_0$  of the order of 150 MPa) when compacted at 5% water content.

The data from specimens of Material B are also plotted (Figure 5) after subtraction of the stiffness of a 'dry' specimen prepared from the bagged constituents and tested without the addition of water, which was found after testing to have a water content of 0.47 %. The variation of stiffness of this specimen (from 40MPa to 110 MPa, see Figure 4) is attributable solely to the influence of net normal stress, so that the values in Figure 5 are due only to suction. Although there is scatter in the data, which appears greater at higher water contents, it is clear that suctions due to lack of saturation play a major role in determining the stiffness of shallow unsaturated

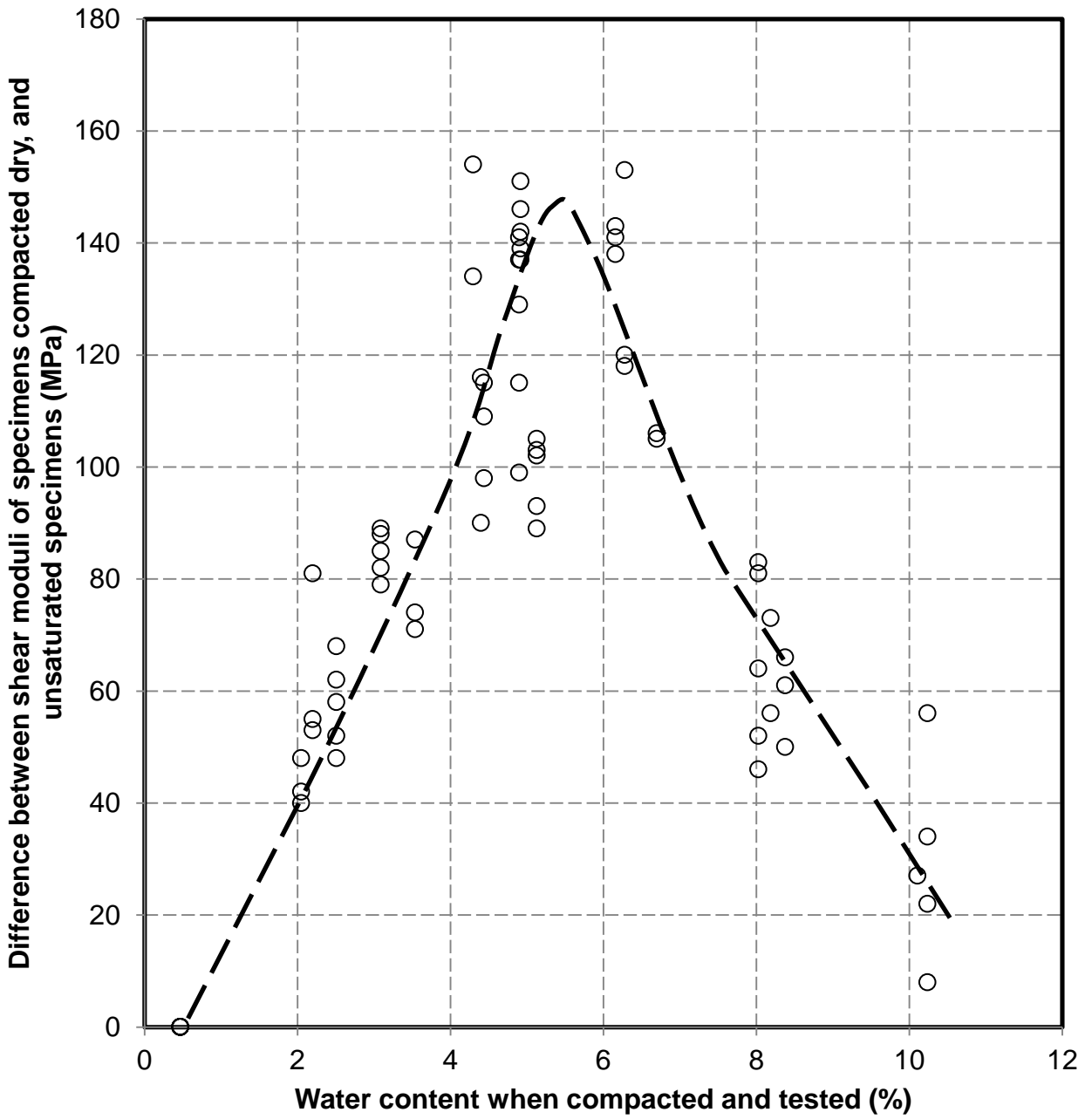


Figure 5. Stiffnesses (shear moduli) from Material B plotted after subtraction of stiffnesses for a specimen compacted and tested dry .

material such as rail formation, where net normal stress levels are generally less than 20-30 kPa.

Figure 4 and Figure 5 also show the effect of net normal stress in increasing small strain stiffness. For dry or saturated sands previous experimental data suggest that shear modulus depends upon mean effective stress:-

$$\left[ \frac{G}{p_a} \right] = a \left[ \frac{\sigma'}{p_a} \right]^b \quad (1)$$

where

$\sigma'$  is the mean effective stress

$p_a$  is a reference pressure (1 kPa, or atmospheric - 100 kPa)

$a$  and  $b$  are material constants, with  $b$  typically of the order of 0.5 for sands [22].

For material B, tested at its as-compacted water content, with net normal stresses between 10 kPa and 150 kPa, individual plots of  $G_0$  as a function of net normal stress gave  $b$  exponents of between 0.24 and 0.56. For tests with applied net normal stresses between 100 kPa and 400 kPa,  $b$  exponent values were higher, and between 0.38 and 0.68.

The assumption that track formation materials will remain at their as-compacted water contents is, of course, unlikely to be true in practice. In arid environments it could be expected to dry out completely. The results of experiments compacted at water contents between 6 % and 10 %, and then air dried are shown in Figure 6. Changes in degree of saturation after compaction can clearly have a large effect on stiffness. These results suggest that if the formation could be laid in a saturated state and dried out (which would clearly be extremely difficult in practice, because of the very low stiffness and strength of the material at low net normal stress levels, which would cause difficulty during compaction) then it would have excellent stiffness properties.

The  $b$  exponents of these specimens, between 0.02 and 0.05, suggest that the high dry stiffness results from structure, because stiffness is not significantly affected by net normal stress. Figure 4 shows maximum small strain stiffness ( $G_0$ ) values of the



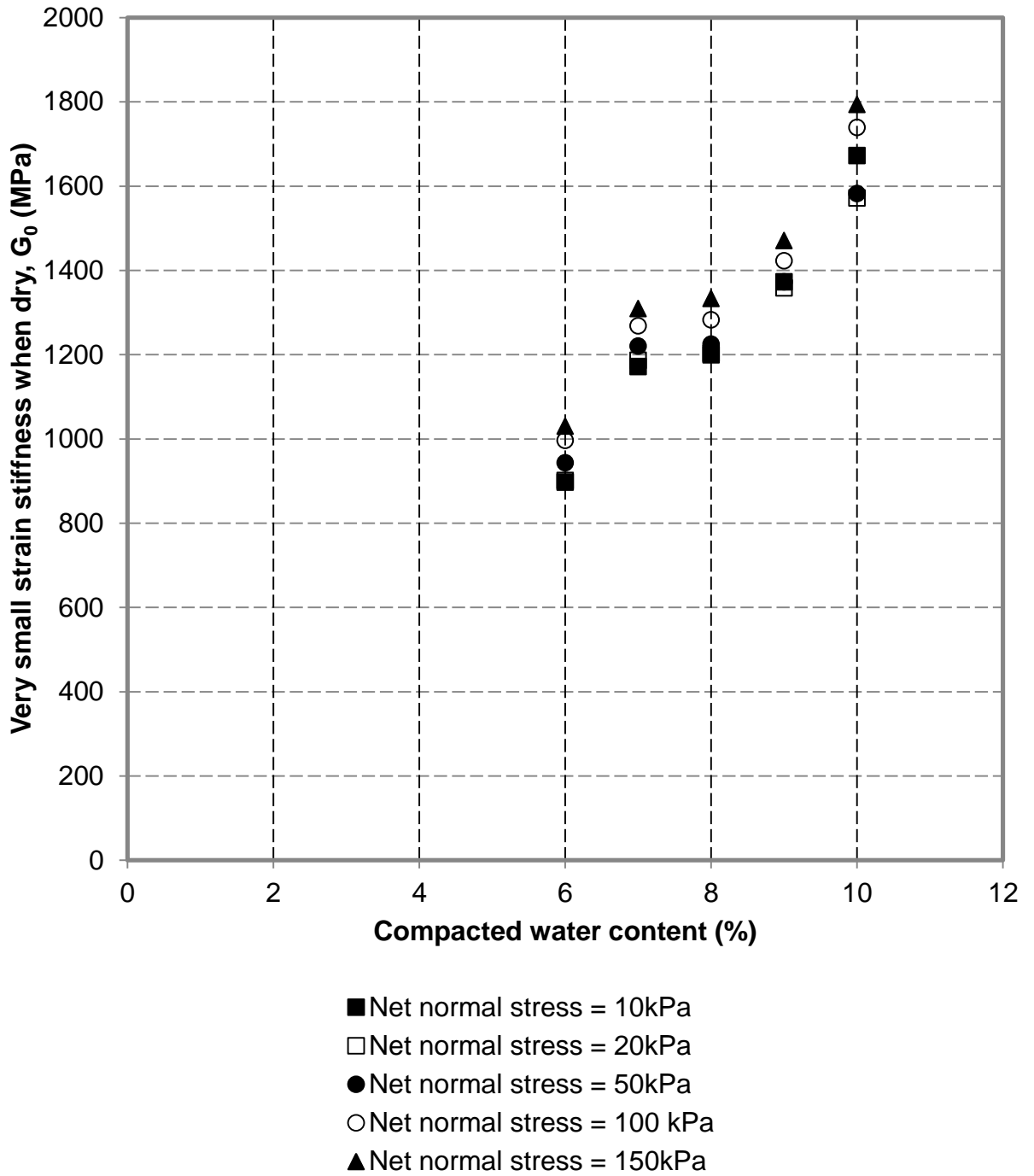


Figure 6. Very small strain stiffness of Material B, compacted at various water contents, and subsequently dried before testing.

order of 150 MPa to 250 MPa for specimens tested at their as-compacted water content, with varying net normal stress. In comparison the minimum stiffness values (for a specimen dried from 6% water content at compaction) in Figure 6 are of the order of 900 MPa to 1800 MPa.

### ***Estimates of matric suction***

It is clear that the materials tested in this study can receive a significant contribution to their small strain stiffnesses in the form of structure resulting from matric suction, as a result of their lack of saturation. However, the pattern of behaviour is complex.

For material compacted and tested at the same water content the effect of matric suction is greatest at small to medium air void contents. Test results suggest that the contribution of lack of saturation to the stiffness of these specimens depends not only upon the value of the matric suction at the time of testing, but also on the fabric set up during compaction [23]. Very low suctions exist at near-saturation water contents. At intermediate water contents suctions are larger, and these have a significant effect on stiffness. But at low water contents, where suctions are at their greatest, they appear (for the material tested here) to make almost no contribution to stiffness. This may be partly because when wetted and compacted in this way the fine fraction of clay and silt forms into clumps (see Figure 3) reducing the effect on the overall specimen stiffness.

The results for material compacted at high water content and then dried are very different. Stiffness seems greatly affected by matric suction, and its variation with compacted water content is presumed to be a reflection of the more uniform distribution of fines within specimens formed in this way.

Figure 7 shows matric suctions for Material B, measured using the filter paper technique, the pressure plate apparatus, and a Ridley suction probe [17]. The pressure plate apparatus and the suction probe are restricted to measurement of matric suction up to 1000 - 1500 kPa, beyond which the filter paper data must be relied upon. It can be seen that the pressure plate and filter paper tests give similar trends whilst, perhaps because of the effect of the soft kaolin paste used to bed the instrument on the specimen, the suction probe gives lower matric suctions at any

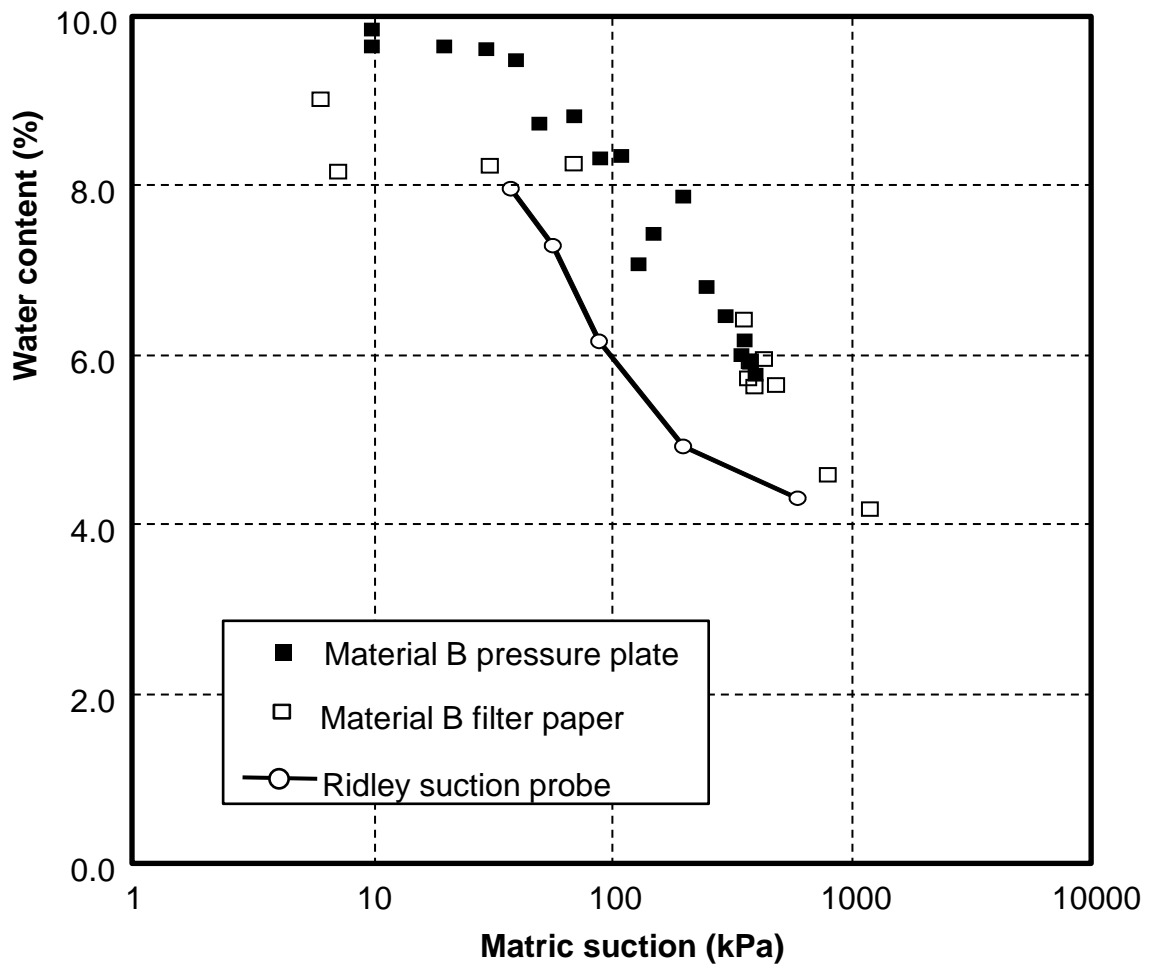


Figure 7. Matric suction as a function of water content for Material B.

given water content. The differences between suctions measured using the three techniques are large - note that the matric suction data in Figure 7 are plotted to a log scale. It is not possible to say which method is best because the true values of suction are unknown.

There is significant scatter in the data, which may result from the differences in the scale of variability, caused by compaction layering (Figure 2) and clumping of finer grained materials (Figure 3) in our specimens. These types of variability almost certainly occur in the field, and affect different sizes of specimen to different extents.

### **Development of a Suction Stress Characteristic Curve**

Figure 8 shows the measured small strain shear modulus of Material B as a function of applied net normal stress. The lower bound is given by test results on saturated specimens, where the applied stress is the effective stress. Open circles give the results of all other tests, carried out on unsaturated material. It can be seen that matric suction has the potential to increase the shear modulus by about 125 MPa.

Previous research [21] has shown that the effect of matric suction on strength can be determined experimentally, by developing a Suction Stress Characteristic Curve (SSCC) as a function of matric suction, or water content, or degree of saturation. According to this research [21] “suction stress, together with net normal stress, completely defines the effective stress in unsaturated soils”. “The true intergranular or effective stress for unsaturated soils ...consists of the net normal stress, the bonding stress when soil is saturated, and suction stress ...”. Thus for uncemented formation material the effective stress (in the sense of Terzaghi [24]) is the sum of net normal stress and suction stress.

An SSCC is relatively straightforward to produce, being based on the results of conventional saturated tests. As noted [21], there are advantages (for example with regard to in-situ monitoring using TDR) in developing the SSCC in terms of water content. Figure 9 shows the calculated SSCC for the very small strain shear modulus of Material B derived from the results of resonant column testing of specimens at their preparation water contents. The procedure followed was as follows:

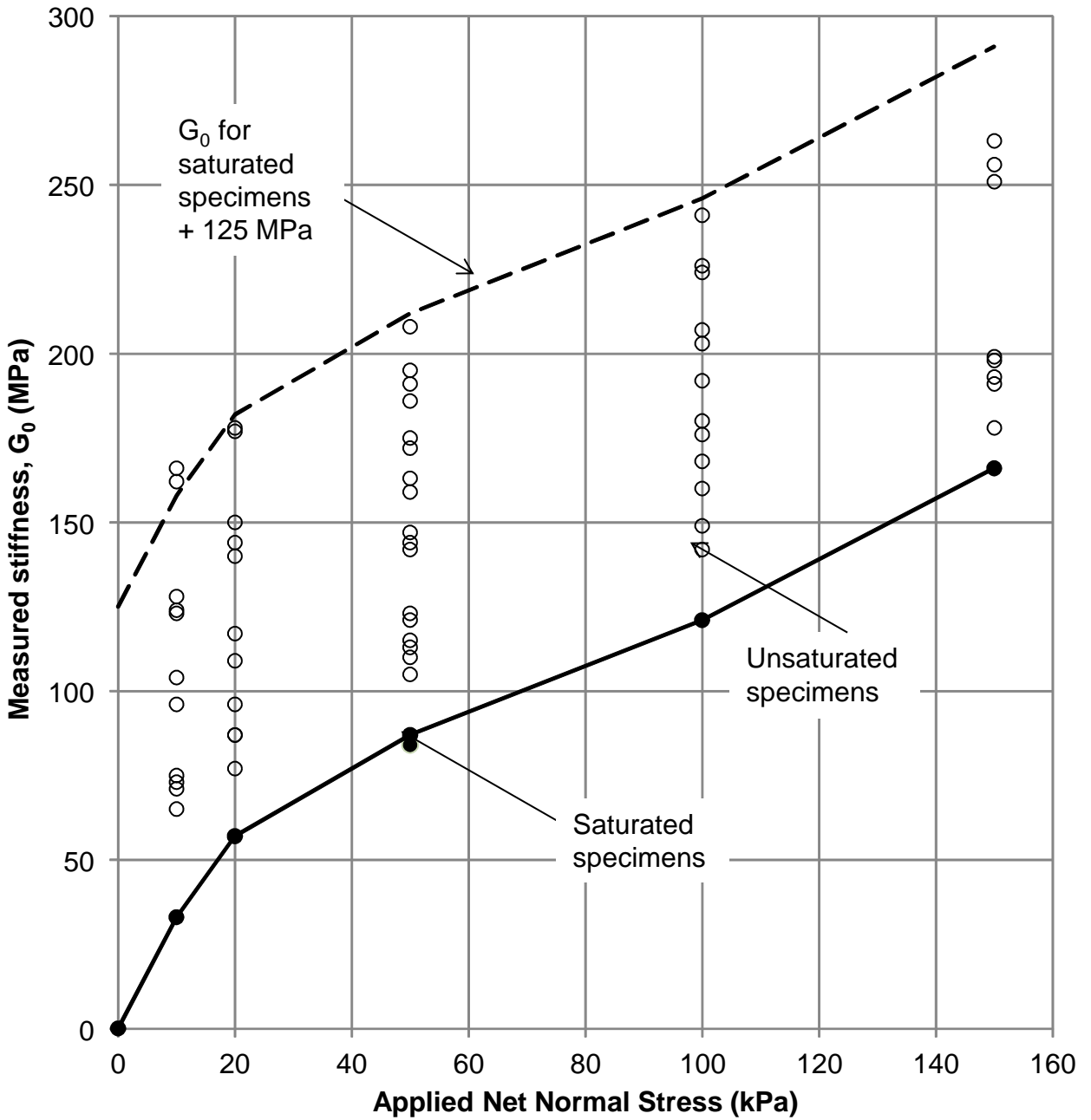


Figure 8. Very small strain stiffness,  $G_0$ , as a function of applied net normal stress, for Material B.

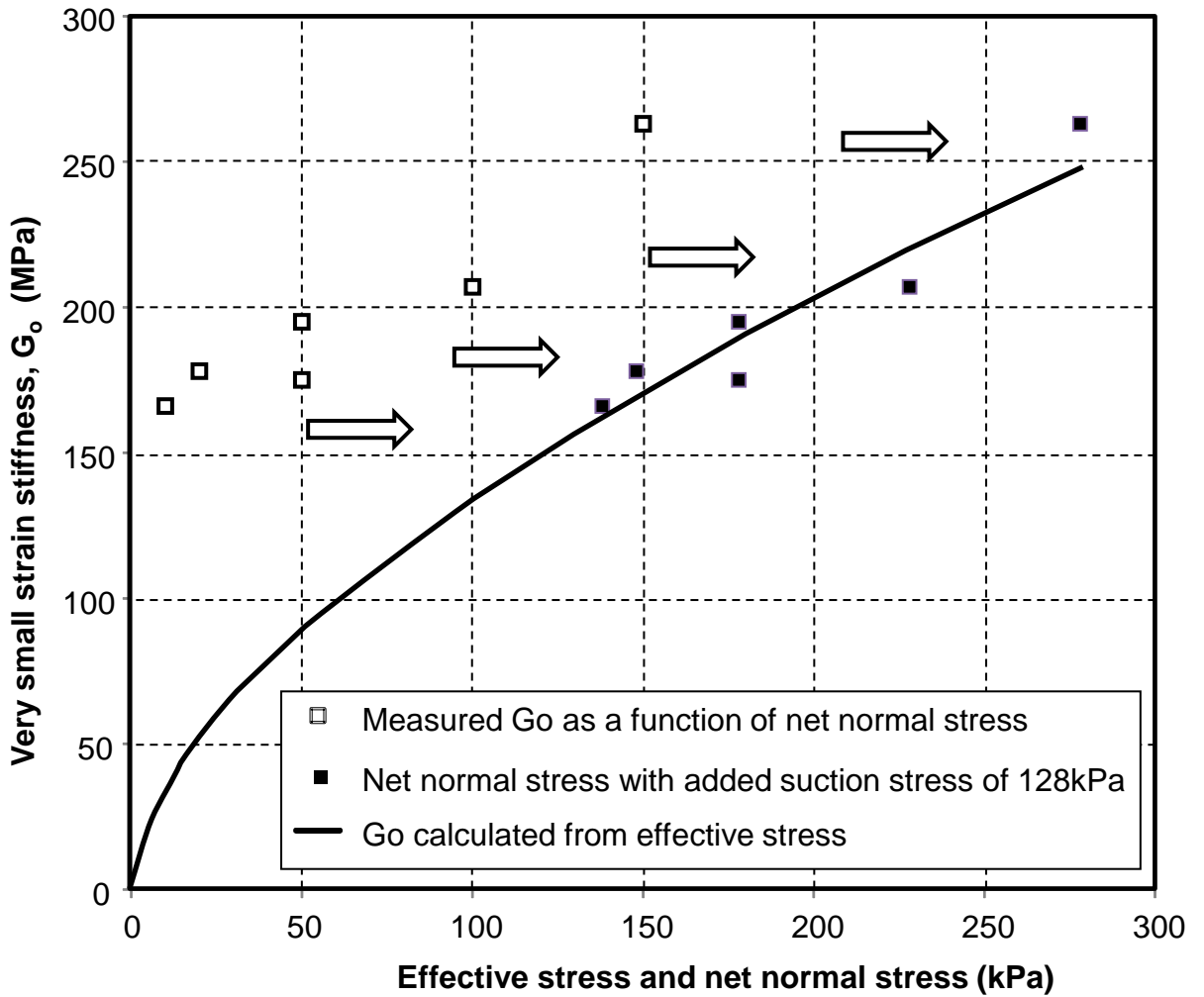


Figure 9. Calculation of suction stress for stiffness data with 6 % water content.

1. The relationship between  $G_0$  and effective stress was determined from the results of resonant column tests on saturated specimens. These are the full black circular points at the bottom of the graph on Figure 8. From these data and Equation (1),  $a = 1350$  and  $b = 0.6$  for  $p_a = 100$  kPa was adopted, for shear modulus, effective stress and net normal stress in kPa.
2. The stiffness data for unsaturated specimens was sorted into 1% intervals of water content – “Calculation method #1” used 2 – 3 %, 3 – 4 %, 4 – 5 %, etc. intervals, whilst “Calculation method #2” used 1.5 – 2.5 %, 2.5 – 3.5 %, 3.5 – 4.5 %, 4.5 – 5.5 %, etc.
3. For each moisture content interval a suction stress was added to the net normal stress, until the sum of the squares of the differences between the calculated and measured shear moduli, in terms of effective stress (net normal stress plus suction stress), was minimised. Figure 9 shows an example where the suction stress at 6 % water content has been calculated as 128 kPa.
4. The suction stresses obtained from minimising the sum of the squares of the errors were plotted as a function of the centre of the water content interval (Figure 10).

The two suction stress characteristic curves differ from each other as a result of the limited data in one or two water content intervals. Nonetheless, the pattern is clear, with a maximum suction stress of the order of 125 kPa occurring at around 6 – 7 % water content. The ability of the SSCC to normalise the stiffness data can be judged from the scatter of the data in Figure 11, where  $G_0$  is plotted as a function of (Net Normal Stress plus Suction Stress).

## CONCLUSIONS

The rational design of rail substructure involves a process of estimating the stiffnesses of the formation materials in the track substructure. Despite numerous empirical and fundamental studies, this task remains a challenge.

The stiffness of the materials used in rail track sub-structures and other shallow infrastructure can be expected to be small when they are saturated, as a result of

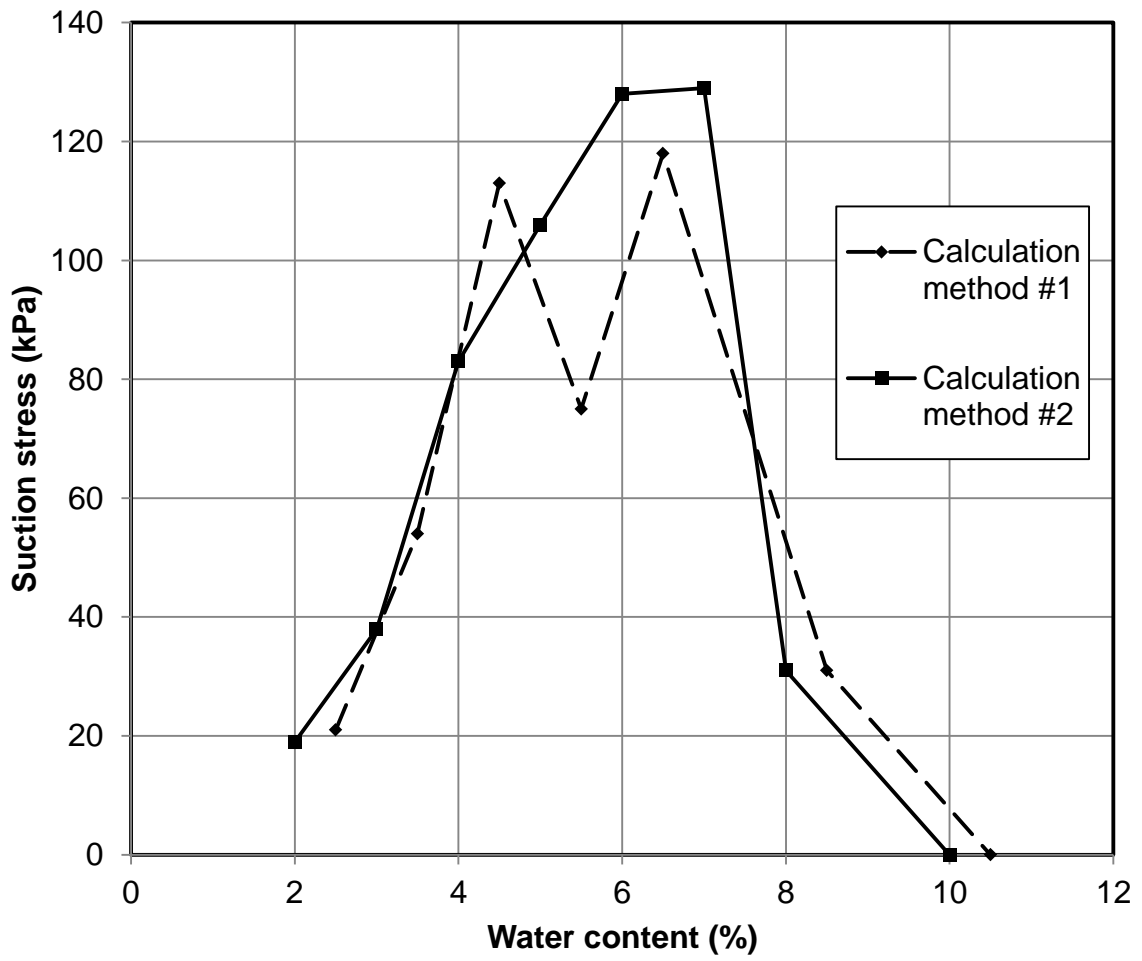


Figure 10. Suction Stress Characteristic Curves for Material B.



their low effective stress levels. Materials compacted and tested dry show similarly low small strain stiffness.

In contrast, unsaturated materials compacted and tested at intermediate water contents can show very much higher stiffness, even at low levels of net normal stress. The magnitude of matric suctions measured at these water contents suggests that they are responsible for increasing stiffness, although other factors, such as fabric and heterogeneity, and strain level will also play a part.

As an example, for Material B, compacted and tested at the same water content, the maximum very small strain shear modulus ( $G_0$ ) increase, which is assumed to result from matric suction, was of the order of 125 MPa at 5% water content.

For material compacted and tested at the same water content, at constant dry density, an optimal water content exists at which maximum stiffness is observed. The value of this can be expected to depend on the composition of the material. Although suction increases with further reduction in water content, for materials compacted and tested at the same water content, it has little effect at low water contents.

In contrast, a series of specimens compacted at varying water contents, air dried to zero water content, then tested for stiffness, showed even larger very small strain stiffnesses. These varied from about 900 MPa when compacted at 6 % water content to 1800 MPa for material compacted at 10% water content (saturation). These specimens showed stiffness which has very little dependency on net normal stress. This suggests that compaction close to saturation produced a fabric that, when dried, was able to provide significant structure to the specimens.

The very small strain stiffness data obtained from resonant column testing of Material B at the as-compacted water content was successfully normalised using an adaptation of the Suction Stress Characteristic Curve method. This was found to be relatively easy to apply, and did not require the development of a Soil Water Characteristic Curve. It should provide a valuable way of generalising stiffness data when carrying out numerical modelling for track design.

## ACKNOWLEDGEMENTS

The work described in this paper was funded by the Engineering and Physical Sciences Research Council's "Rail Research UK" programme, and was supported by the University of Southampton's School of Civil Engineering and the Environment. The authors are also grateful to Dr. Andrew Ridley of Geotechnical Observations Ltd. U.K. for the use of his suction probe apparatus.

## REFERENCES

1. Li, D. and Selig, E.T. (1998) Method for railroad track foundation design. II Applications. *J. Geotech. Geoenv. Engng*, 124, 4, 323-329.
2. Li, D. and Selig, E. T. (1994). Resilient modulus for fine-grained subgrade soils, *Journal of Geotechnical Engineering*, ASCE, Vol. 120 No. 6, 939 - 957.
3. Gräbe, P.J. and Clayton, C.R.I. (2009). Effects of principal stress rotation on permanent deformation in railway track. *J. Geotech. Geoenv. Engng*, 135, 4, 555-565.
4. Gräbe, P.J. and Clayton, C. R. I. (2014). "Effects of principal stress rotation on resilient behavior in rail track foundations." *J. Geotech. Geoenviron. Eng.*, 140, 2, 04013010-1 - 04013010-10. DOI: 10.1061/(ASCE)GT.1943-5606.0001023
5. Lourens, J.P. and Maree, J.S. (1997). Rehabilitation Design of High Embankments and a Coal Line Track Formation. *Proc.6th Int. Heavy Haul Conf.*, Cape Town, South Africa.
6. Gräbe, P.J., Clayton, C.R.I. and Shaw, F.J. (2005). Deformation measurement on a heavy haul track formation. *Proc. 8th Int. Heavy Haul Conf.*, Rio de Janeiro, Brazil, 287-295.
7. Mancuso, C., Vassallo, R. and d'Onofrio, A. (2002). Small strain behaviour of a silty sand in controlled-suction resonant column torsional shear tests. *Canadian Geotech. J.*, 39, 1, 22-31.
8. Mancuso, C., Vassallo, R. and d'Onofrio, A. (2003). Small strain behaviour of soils in controlled suction conditions. *Proc. 3rd Int. Conf. on Unsaturated Soils*, Recife, Brazil, 3, 917-928.

9. Dineen K., Colmenares J.E., Ridley, A.M. and Burland J.B. (1999). Suction and volume changes of a bentonite-enriched sand. *Proc. ICE - Geotechnical Engineering*, 137, Oct ., 197-201.
10. Frost, J.D. and Park, J.Y. (2003). A critical assessment of the moist tamping technique. *Geotechnical Testing J.*, 26, 1, 57-70.
11. Anderson, D.G. and Stokoe, K.H. II (1977). Shear modulus: a time dependent soil property. In 'Dynamic Geotechnical Testing'. ASTM STP 654, 66-90.
12. Clayton, C.R.I., Priest, J.A., Bui, M., Zervos,A., and Kim, S.G. (2009). The Stokoe resonant column apparatus: effects of stiffness, mass and specimen fixity. *Géotechnique*, 59, 5, 429-437.
13. Chandler, R.J. and Gutierrez, C.I. (1986). The filter paper method of suction measurement. *Géotechnique*, 36, 2, 265-268.
14. ASTM D5298-4 (1994). Standard test method for measurement of soil potential (suction) using filter paper. ASTM, Philadelphia, USA.
15. ASTM D6836-02 (2003). Standard test methods for determination of the soil water characteristic curve for desorption using a hanging column, pressure extractor, chilled mirror hygrometer and/or centrifuge. ASTM, Philadelphia, USA.
16. Ridley, A.M. and Burland, J.B. (1993). A new instrument for the measurement of soil moisture suction. *Géotechnique*, 43, 2, 321-324.
17. Leong, E.C., He, L., and Rahardjo, H. (2002). Factors affecting the filter paper method for total and matric suction measurements. *Geotech. Testing J.*, 25, 3, 322-333.
18. Chandler, R.J., Crilly, M.S., and Montgomery-Smith, G. (1992). A low-cost method of assessing clay desiccation for low-rise building. *Proc. ICE – Geotechnical Engineering*, 92, 2, 82-89.
19. Ridley, A.M. (pers. com.). Results of measurements of suction using the Ridley suction probe. Geotechnical Observations Ltd., Weybridge, Surrey U.K.
20. Lu, N. and Likos, W.J. (2006). Suction Stress Characteristic Curve for unsaturated soil. *J. Geotech. Geoenv. Engng*, 132, 2, 131-142.
21. Heath, A.C., Pestana, J.M., Harvey, J.T. and Bejerano, M.O. (2004). Normalizing behaviour of unsaturated granular pavement materials. *J. Geotech. Geoenv. Engng.*, 130, 9, 896-904.

22. Clayton, C.R.I. (2011). Stiffness at small strain: research and practice. *Géotechnique*, 61, 1, 5-37.
23. Seed, H.B., Chan, C.K. and Lee, C.E. (1962) Resilient characteristics of subgrade soils and their relation to fatigue failures in asphalt pavements. Proc. Int. Conf. on Structural Design of Asphalt Pavements, University of Michigan, Ann Arbor, Michigan, August, 611-636.
24. Terzaghi, K. (1943). *Theoretical Soil Mechanics*. John Wiley, New York.